RESEARCH

Interventional effects of the direct application of "Sanse powder" on knee osteoarthritis in rats as determined from lipidomics via UPLC-Q-Exactive Orbitrap MS

Peng Wu[1,2,5†], Zhengquan Huang[1,2†], Jinjun Shan[3,4], Zichen Luo[3,4], Nongshan Zhang[1,2], Songjiang Yin[1,2], Cunsi Shen[3,4], Runlin Xing[1,2], Wei Mei[1,2], Yancheng Xiao[1,2], Bo Xu[1,2], Jun Mao[1,2*] and Peimin Wang[1,2*]

Abstract

Background: Our previous clinical evidence suggested that the direct application of "Sanse powder" the main ingredient of "Yiceng" might represent an alternative treatment for knee osteoarthritis. However, the mechanism underlying its effect is poorly understood. In this study, we investigated the mechanism of the effect of direct "Sanse powder" application for the treatment of knee osteoarthritis (KOA) in rats by using lipidomics.

Methods: KOA rats were established by cutting the anterior cruciate ligament, and the cold pain threshold and mechanical withdrawal threshold (MWT) of seven rats from each group were measured before modelling (0 days) and at 7, 14, 21 and 28 days after modelling. Histopathological evaluation of the synovial tissue was performed by haematoxylin and eosin (H&E) staining after modelling for 28 days. Interleukin-1β (IL-1β), pro-interleukin-1β (pro-IL-1β) and tumor necrosis factor-α (TNF-α) proteins in synovial tissue were measured by western blot, and the mRNA expression levels of IL-1β and TNF-α in synovial tissue were measured using Real-time reverse transcription polymerase chain reaction (qRT-PCR), the levels of IL-1β and TNF-α in rat serum were measured by enzyme-linked immunosorbent assay (ELISA), Serum lipid profiles were obtained by using ultra-performance liquid chromatography combined with quadrupole-Exactive Orbitrap mass spectrometry (UPLC-Q-Exactive Orbitrap MS).

Results: The results confirmed that the direct application of "Sanse powder" had a significant protective effect against KOA in rats. Treatment with "Sanse powder" not only attenuated synovial tissue inflammation but also increased the levels of the cold pain threshold and MWT. In addition, the lipidomics results showed that the levels of diacylglycerol (DAG), triacylglycerols (TAGs), lysophosphatidylcholine (LPC), phosphatidylcholine (PC), fatty acid esters of hydroxy fatty acids (FAHFAs), and phosphatidylethanolamine (PE) were restored almost to control levels following treatment.

Conclusions: Lipidomics provides a better understanding of the actions of direct application "Sanse powder" therapy for KOA.

*Correspondence: junmao1978@hotmail.com; drwpm@163.com
†Peng Wu and Zhengquan Huang contributed equally to this work
[1] Affiliated Hospital of Nanjing University of Chinese Medicine, Nanjing 210029, China
Full list of author information is available at the end of the article

Wu *et al. Chin Med*   (2020) 15:9

Page 2 of 13

Background

Increasing research suggests that knee osteoarthritis (KOA) is a total joint disease involving cartilage, subchondral bone, ligaments, the meniscus and the synovium [1]. Synovial inflammation may be important in the pathogenesis of KOA and is associated with pain. To date, there is no specific treatment for KOA [2]. Pharmacological therapy may include the paracetamol, non-steroidal anti-inflammatory drugs (NSAIDs) or intra-articular corticosteroids, However, the long-term use of NSAIDs can lead to adverse reactions, such as peptic ulcers and bleeding, and although selective COX-2 inhibitors can effectively reduce the incidence of similar events, they can have adverse effects on the cardiovascular system [3–5].

Many studies have shown significant treatment effects of traditional Chinese medicine on KOA. "Sanse powder" is the main component of "Yiceng", and our previous studies found that "Yiceng" application alleviated synovial inflammation, relieved pain and improved the cold pain threshold [6, 7]. However, the mechanisms underlying these effects remain unclear.

The close relationship between lipid metabolism and KOA has attracted widespread attention. Lipid metabolism imbalance can induce KOA, and KOA can also lead to lipid metabolism disorders. Lipidomics is increasingly recognized as an invaluable tool for identifying changes in lipid metabolites and reveal the underlying mechanisms [8, 9]. As there are many kinds of lipids and as the substrates of biological samples are complex, so the analysis of lipidomics requires advanced separation technology and detection. Liquid chromatography-tandem mass spectrometry (LC-MS) is effective for the analysis of lipids in biological samples. Ultra-performance liquid chromatography (UPLC) enables the rapid and effective separation of individual lipid species. Lipidomics based on UPLC combined with quadrupole-Exactive Orbitrap mass spectrometry (UPLC-Q-Exactive MS) has been widely applied to obtain insight into many biological events [10]. In this study, UPLC-Q-Exactive MS was used to analyse various lipids in the serum of KOA rats treated with "Sanse powder". An experiment was conducted to evaluate the effects of adhesive "Sanse powder" treatment on the lipid profile. The results provide a new understanding of the effects of this treatment for KOA.

Methods

Preparation of "Sanse powder" patches

"Sanse powder" patches were created from eleven Chinese material medica (CMMS), *Forsythia suspensa*, Glycyrrhiza uralensis, Salvia miltiorrhiza, *Gentiana macrophylla*, Chaenomeles sinensis, *Strychnos nux-vomica*, Ligusticum striatum Hort, *Curcuma longa*, Paeonia lactiflora, Notopterygium root and Saposhnikovia divaricata, all at equal ratios. All of the CMMs were purchased from Anhui Wansheng Traditional Chinese Medicine Decoction Pieces Co., Ltd., (Anhui, China) and authenticated by Professor Peimin Wang from Affiliated Hospital of Nanjing University of Chinese Medicine (Nanjing, China). All the herbal materials used in our study satisfy the quality requirements of the 2015 edition of the Chinese Pharmacopoeia. All the herbs were ground into powder and mixed with Vaseline at a 1:1 ratio to create the patches.

Animals

Twenty-one male Sprague–Dawley rats weighting 150 g to 180 g were purchased from Nanjing Qinglongshan Animal Farm (animal certificate number: SCXK-Zhe-2014-0001). All animal procedures were performed in accordance with the Guidelines for Care and Use of Laboratory Animals of Nanjing University of Chinese Medicine. The rats were housed in an environment with a room temperature of 24–26 °C, a relative humidity of 55%, and a 12-h light–dark cycle. The experiments were approved by the Animal Ethics Committee of Nanjing University of Chinese Medicine. The project identification code of the ethical statement is 201810A001 (Additional file 1).

One week after adaptive feeding, the rats were randomly grouped into three groups: a control group (n=7), a KOA group (n=7), and a "Sanse powder" group (KOA+Sanse powder, n=7). The KOA model was constructed by anterior cruciate ligament transection (ACLT) surgery, as described previously, on both knees [11]. The drug was administered to the "Sanse powder" group after preparation of the KOA model. The knees were skinned and "Sanse powder" paste (0.8 g/10 cm^2) was evenly applied to the skin surface for 8 h a day for a total of 14 days. After the 14 days, the rats were sacrificed to harvest the cartilage, synovial tissue and plasma.

Sample collection

After the final treatment administration, the rats were anaesthetized by intraperitoneal injection with 3% pentobarbital sodium and sacrificed after sampling blood from the abdominal aorta (CO$_2$ asphyxiation). The knees were skinned close to the patellar ligament on both sides of the cut and the superior border of the patella. A distal lateral incision in the quadriceps was made to the femur, and the

Wu *et al. Chin Med*   (2020) 15:9

Page 3 of 13

patella and its surrounding tissues were obtained with ophthalmic forceps. The surgical blade was manipulated carefully to avoid damaging the transparent synovial tissue. The synovial tissue from two randomly selected rats from each group was preserved in 4% paraformaldehyde for pathological section, and the remaining the synovial tissues from the groups were cryopreserved at −80 °C.

Histopathology

After 2 weeks, cartilage was taken from the control and model KOA groups, fixed in 10% neutral formalin, embedded in paraffin cut into slices, and stained by haematoxylin and eosin (H&E) staining. After 14 days of administration, rats were sacrificed to harvest the synovial tissue and serum, and the synovial tissue was treated as cartilage.

Measurements of inflammatory mediators
Western blotting

Western blotting was performed as previously described [12]. The blots were incubated with primary antibodies, including anti-IL-1β (1:1000, Abcam, Cambridge, UK), anti-pro-IL-1β (1:1000, Abcam, Cambridge, UK) and anti-TNF-α (1:1000, Abcam, Cambridge, UK).

Real-time reverse transcription polymerase chain reaction (qRT-PCR)

qRT-PCR was performed as previously described [12]. Primer was designed and synthesized by Shanghai Biotechnology Service Company in accordance with Gene sequence in GenBank Gene sequence design, together with Oligo v6.6. Sequences for primes were as follows: TNF-α forward, 5'-TGGGCTCCCTCTCATCAGTTC-3' and reverse, 5'-GCTCCTCCGCTTGGTGGTTTG-3'; IL-1β forward, 5'-ACAGCAGCATCTCGACAAGAGC-3' and reverse, 5'-CCACGGGCAAGACATAGGTAGC-3'; GAPDH forward, 5'-GATGCTGGTGCTGAGTATG-3' and reverse, 5'-GTGGTGCAGGATGCATTGCT-3'.

Enzyme-linked immunosorbent assay (ELISA)

The leves of IL-1β and TNF-α in rat serum were estimated using a rat ELISA kit (FcMACS, Nanjing, China) according to manufacturer instructions.

Measurements of the cold pain threshold and mechanical withdrawal threshold (MWT)
Cold pain threshold

Cold pain sensitivity was determined at 0, 7, 14, 21, and 28 days after modelling, The measurement was performed at 7:00 AM by placing a rat on a cold plate (35150-001, Ugo Basil SLR, Italy) with a temperature of 0 ± 3 °C [13], covering the rats with an organic cylinder and recording the time from contact with the cold plate to the time of rat rapid paw withdrawal, paw licking, foot stamping or jumping; paw withdrawal due to physical activity was not considered a positive reaction. The measurement was performed 3 times with 10 min between each test, and the average value was obtained.

MWT

The MWT was measured at 0, 7, 14, 21, and 28 days after modelling. Measurements were taken at 14:00, and all rats were acclimated to the testing environment 5 min before the test. The rats were placed in Plexiglass cages with wire mesh (BME-404, Institute of Biomedical Engineering, Chinese Academy of Medical Sciences). An electronic needle was used to stimulate the sole of the right hind foot. The stimulation intensity was increased gradually with the needle gradually bending until the rats exhibited rapid paw withdrawal, lifting, and licking reactions within 3 s. A computer automatically displayed the minimal force on the needle to induce paw withdrawal. The measurement was made 3 times, with 10 min between each test, and the average value was obtained.

Processing and determination of "Sanse powder"

One gram of "Sanse powder" was placed in a conical flask with 25 mL methanol. After 45 min of ultrasonic oscillation, the extract was centrifuged at 18,000 rpm, and the supernatant was used for mass spectrometric analysis. The following standards were used: curcumin (32.24 µg/mL), ligustilide (32.63 µg/mL), tanshinone I (28.03 µg/mL), imperatorin (32.89 µg/mL), gentiopicroside (34.34 µg/mL), osthole (35.66 µg/mL), oleanolic acid (31.18 µg/mL), quercetin (35.13 µg/mL), and paeoniflorin (33.42 µg/mL). The standards were mixed together to create a standard solution, and the fragment ions and retention time were compared with those of samples by chromatographic and mass spectrometric analysis.

A UPLC instrument (Waters, USA) was used to separate the samples. Acetonitrile (A) and 0.1% aqueous formic acid (B) were selected as the mobile phases. The gradient mobile phase programme was as follows: 0 min, 10% A; 50 min, 90% A; 52 min, 90% A; 55 min, 10% A; and 60 min, 10% A. The column oven temperature was 25 °C, and the flow rate was 0.4 mL/min. A Hypersil GOLD column (100 × 2.1 mm, Thermo, USA) was used.

An LTQ-Orbitrap XL mass spectrometer was used to analyse the samples, and the detection conditions were the same in both positive and negative ion modes. The sheath gas flow rate and aux gas flow rate were 45 arb and 10 arb, respectively. The heater temperature and capillary temperature were both 300 °C, and the capillary voltage was 35 V.

Wu *et al. Chin Med*   (2020) 15:9

Page 4 of 13

Analysis conditions of UPLC-Q-Exactive MS
Treatment of the serum samples of KOA rats

Serum was thawed to 4 °C, and 20 µL of serum was placed into a 1.5 mL centrifuge tube, to which 225 µL of cold methanol was added. The internal standard (lyso-PE (17:1), SM (17:0), Avanti Polar Lipids, United States, approximate concentration: 5 µg/mL) was also added. The mixture was vortexed (Scientific Industries, USA) for 10 s, and 750 µL MTBE was added. The mixture was vortexed for 10 s and then oscillated for 10 min at 4 °C. Ultrapure water (188 µL) was then added, and the mixture was vortexed for 20 s and then centrifuged at 18,000 rpm Beckman, USA for 2 min at 4 °C. A total of 350 µL of the supernatant solution was placed into a 1.5 mL centrifuge tube, which was placed in a centrifuge concentrator (Thermo, USA). The samples were redissolved in 110 µL of methanol: toluene (9:1), vortexed for 10 min, and sonicated (Kunshan Ultrasonic Instrument Co., Ltd.). The samples were then centrifuged for 10 min at 18,000 rpm, and samples of the supernatant were collected for analysis.

The QC samples were prepared by combining 10 µL samples in the same centrifuge tube, and 20 µL of sample were then collected and treated according to the above experimental steps.

Chromatographic conditions

A U3000 high-performance liquid chromatograph (Dionex, USA) was used to separate the samples and was equipped with an ACQUITY CSH C18 column (1.7 µm, 2.1×100 mm). The flow rate was 0.3 mL/min, and the mobile phase in positive ion mode was (A) 6:4 acetonitrile: water + 10 mM ammonium formate + 0.1% formic acid and (B) 9:1 isopropanol: acetonitrile + 10 mM ammonium formate + 0.1% formic acid. The mobile phase in negative mode was (A) 6:4 acetonitrile: water + 10 mM ammonium acetate and (B) 9:1 isopropanol: acetonitrile + 10 mM ammonium acetate. The gradient of the mobile phase was as follows: 0–2 min, 15–30% B; 2–2.5 min, 30–48% B; 2.5–11 min, 48–82% B; 11–11.5 min, 82–99% B; 11.5–12 min, 99% B; 12–12.1 min, 99–15% B; and 12.1–15 min, 15% B. The column temperature was 65 °C, and the injection volume was 2 µL in both positive and negative ion mode.

Mass spectrometric conditions

A Q-Exactive four-stage pole-orbit well mass spectrometer (Thermo Fisher Scientific) was used to detect samples. A hybrid quadrupole-Exactive Orbitrap mass spectrometer was coupled to an HESI source. The instrument parameters for position ion mode were as follows: spray voltage, 3.5 kV; heater temperature, 306 °C; capillary temperature, 300 °C; sheath gas flow, 45 arb; aux gas flow, 10 arb; scanning range, 215–1800 m/z; and s-lens, 50. The parameters for negative mode were as follows: spray voltage, 3.0 kV; heater temperature, 325 °C; capillary temperature, 300 °C; sheath gas flow, 45 arb; aux gas flow, 10 arb; scanning range, 215–1800 m/z; and s-lens, 50.

Data processing method

Using the software Abf Converter (http://www.reifycs.com/AbfConverter/), the raw files were converted into Abf format, and the positive and negative ion mode data were imported into MS-DIAL software for data preprocessing, filtering, alignment and peak identification. Related software parameters are listed in the following table. The identified metabolites, retention times (Rt), mass-to-charge ratios (m/z) and high peak value information were obtained for all samples. The data exported from MS-DIAL were normalized by the SERRF algorithm through the R language. The R language was used to compare FCs with the median peak height of each group. An FC > 1.5 was considered to indicate a significantly difference. Non-parametric analysis and FDR analysis were used to analyse the differences between groups and obtain *P* values. An FDR-adjusted $P < 0.05$ was considered to indicate significance. Using Metaboanalyst (http://www.metaboanalyst.ca/), data on principal component analysis and cluster analysis were conducted.
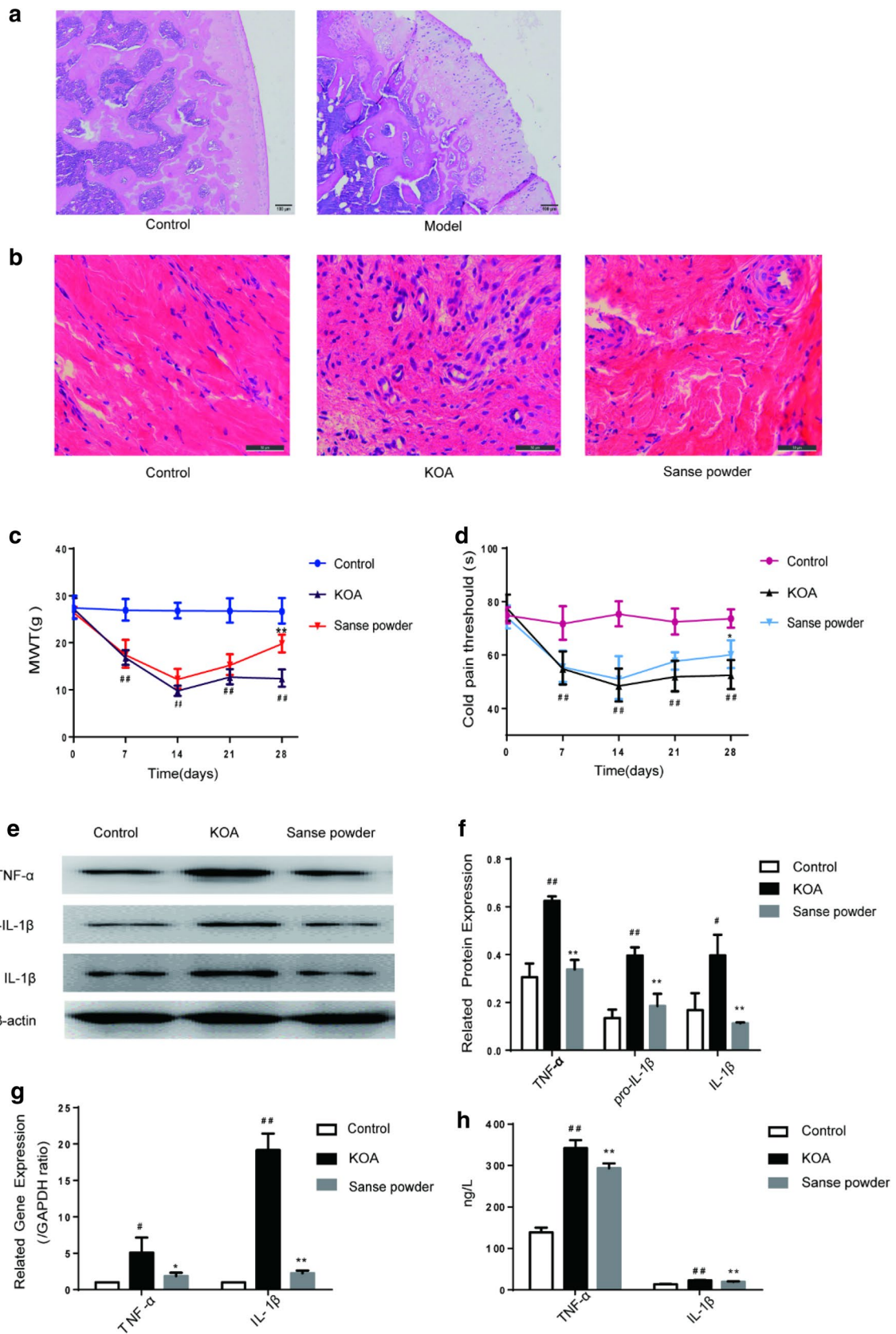
Results
"Sanse powder" can alleviate the symptoms of KOA

After 14 days of modelling, 1 rat from each of the control group and the model group was selected randomly. Histopathology analysis of the cartilage of rats (Fig. 1a) in the control and model groups was performed to confirm that the KOA model had been successfully established. In the control group, the cartilage surface was smooth with no cracks or defects, and the chondrocytes were arranged in an orderly manner, with normal structural layering and

---

(See figure on next page.)

Fig. 1 "Sanse powder" can alleviate the symptoms of KOA. Notes. **a** Cartilage histomorphology of each group stained with H&E, 40×, scale bar = 100 µm. **b** Representative synovial tissues of each group stained with H&E, 400×, scale bar = 50 um. **c**, **d** MWT and cold pain threshold of each group. [#]*P* < 0.05, [##]*P* < 0.01 vs. control group; *P* < 0.05, **P* < 0.01 vs KOA group (n = 7). **e**, **f** Representative protein bands for each group. [#]*P* < 0.05, [##]*P* < 0.01 vs. control group; *P* < 0.05, **P* < 0.01 vs. KOA group. **g** Representative gene bands for each group. [#]*P* < 0.05, [##]*P* < 0.01 vs. control group; *P* < 0.05, **P* < 0.01 vs. KOA group. **h** Levels of TNF-α and IL-1β in rat serum were detected by ELISA. [#]*P* < 0.05, [##]*P* < 0.01 vs. control group; *P* < 0.05, **P* < 0.01 vs. KOA group

Wu *et al. Chin Med* (2020) 15:9

Page 5 of 13

Wu *et al. Chin Med*   (2020) 15:9

Page 6 of 13

uniform staining. In the model group, the cartilage sur-face was severely altered and had many cracks, with some extending down to the radiation layer, and exhibited unclear stratification, an irregular structure of each layer and pronounced thickening of the calcification layer. In the HE staining section of the synovial membrane, the cells in the control group were arranged in an orderly manner, with almost no inflammatory cell infiltration. In the model group, inflammatory cell infiltration was sig-nificantly increased, the synovial cells had proliferated to large numbers and were irregularly arranged, and defects were apparent around the synovial tissue, presenting pathological changes of severe synovitis. The infiltration of inflammatory cells in the "Sanse powder" group was significantly reduced related to that in the KOA group (Fig. 1b). We also observed that "Sanse powder" treat-ment increased the cold pain threshold and MWT in KOA rats (Fig. 1c, d). We also analysed the relative pro-tein and gene expressions in synovial tissue and the levels of TNF-α and IL-1β in the rat serum. The results showed that the "Sanse powder" group exhibited significant downregulation of those proteins relative to the expres-sion in the KOA group (Fig. 1e–h).

Chemical constituents of "Sanse powder" prescription

By comparing the accurate m/z and mass fragmentation pattern with those in the literatures, thirty-five compo-nents were tentatively identified by LTQ-Orbitrap MS, including curcumin, ligustilide, and tanshinone I. The base peak chromatogram of the extract of "Sanse pow-der" is depicted in Fig. 2, and a summary of lipid metabo-lites detected by LTQ-Orbitrap MS is shown in Table 1. The compounds detected were divided into several cat-egories, including alkaloids, saponins, lactones, and organic acids. Six ingredients from Forsythia suspensa were identified. Three ingredients were from Glycyrrhiza uralensis, six ingredients were from Salvia miltiorrhiza, four ingredients were from Gentiana macrophylla, three ingredients were from Chaenomeles sinensis, four ingre-dients were from Strychnos nux-vomica, five ingredients were from Ligusticum striatum Hort, one ingredient was from Curcuma longa, one ingredient was from Paeonia lactiflora, one ingredient was from Notopterygium root and one ingredients was from Saposhnikovia divaricata. Most of the ingredients have been reported possess anti-inflammatory and analgesic activity. For example, genti-opicroside exerted anti-inflammatory effects in vivo by inhibiting prostaglandin E2 (PGE2) release and type II
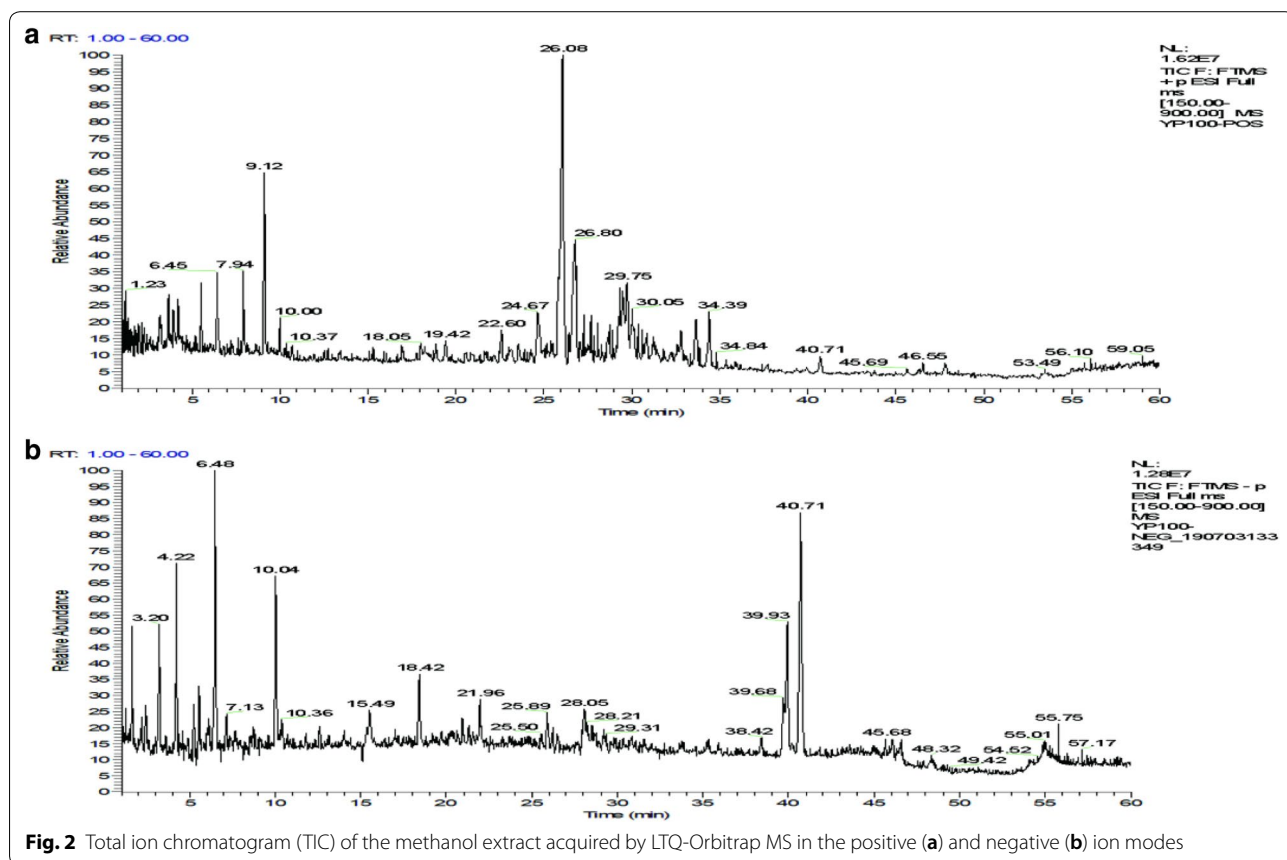

Fig. 2 Total ion chromatogram (TIC) of the methanol extract acquired by LTQ-Orbitrap MS in the positive (**a**) and negative (**b**) ion modes

Wu *et al. Chin Med*   (2020) 15:9

Page 7 of 13

Table 1 The chemical components identified in the "Sanse powder" water extract

(A) positive ion mode

No.	Components	Chemical formula	ESI$^+$, m/z	RT (min)	References
1	Arginine	$C_6H_{14}N_4O_2$	175.11895 [M+H]$^+$, 116.70, 175.19, 71.84	0.63	[21]
2	Gentiopicroside	$C_{16}H_{20}O_9$	357.11800	3.20	*
3	Ferulic acid	$C_{10}H_{10}O_4$	195.06519 [M+H]$^+$, 176.91, 137.88, 120.88	3.20	[21]
4	Strychnine	$C_{21}H_{22}N_2O_2$	335.1754 [M+H]$^+$, 222.04, 234.09, 264.10	3.66	[22]
5	Brucine	$C_{23}H_{26}N_2O_4$	395.19653 [M+H]$^+$ 324.11, 367.17, 350.18	3.99	[22]
6	Strychnine N-oxide	$C_{21}H_{22}N_2O_3$	351.17031 [M+H]$^+$, 334.24, 306.16	4.33	[22]
7	Vomicine	$C_{22}H_{24}N_2O_4$	381.18088 [M+H]$^+$, 324.14, 264.11, 306.17	5.06	[22]
8	Rutin	$C_{27}H_{30}O_{16}$	611.16066 [M+H]$^+$, 257.24, 285.20	6.13	[18]
9	Forsythoside A	$C_{29}H_{36}O_{15}$	647.19464 [M+Na]$^+$, 347.17, 321.13	6.46	[18]
10	Pinoresinol-β-D-glucoside	$C_{26}H_{32}O_{11}$	543.18368 [M+Na]$^+$, 218.93, 289.13	7.10	[18]
11	Phillyrin	$C_{27}H_{34}O_{11}$	557.19933 [M+Na]$^+$, 291.25, 218.96	10.38	[18]
12	Licorice-saponin G2	$C_{42}H_{62}O_{17}$	839.40597 [M+H]$^+$, 487.50, 627.38	16.92	[19]
13	Senkyunolides A	$C_{12}H_{16}O_2$	193.1223 [M+H]$^+$, 193.11, 174.95, 146.96	18.59	[23]
14	Imperatorin	$C_{16}H_{14}O_4$	271.09648	21.80	*
15	Glycycoumarin	$C_{21}H_{20}O_6$	369.13326 [M+H]$^+$, 191.11, 285.09, 148.86	21.67	[19]
16	Curcymin	$C_{21}H_{20}O_6$	369.13326	21.67	*
17	Ligustilide	$C_{12}H_{14}O_2$	191.10665	21.82	*
18	3-Butylphthalide	$C_{12}H_{14}O_2$	191.10665 [M+H]$^+$, 191.07, 144.92, 172.92	21.82	[23]
19	Osthole	$C_{15}H_{16}O_3$	245.11722	23.17	*
20	Cryptotanshinone	$C_{19}H_{20}O_3$	297.14852 [M+H]$^+$, 237.04, 251.65, 279.07	25.89	[20]
21	Tanshinone I	$C_{18}H_{12}O_3$	277.08592	26.15	*
22	Senkyunolides P	$C_{24}H_{30}O_4$	383.22168 [M+H]$^+$, 383.32, 355.25, 365.20	29.75	[23]
23	Tanshinone II A	$C_{19}H_{18}O_3$	295.13287 [M+H]$^+$, 249.13, 277.11	30.06	[20]

(B) Negative ion mode

No.	Components	Chemical formula	ESI$^-$, m/z	RT (min)	References
1	Loganic acid	$C_{16}H_{24}O_{10}$	375.12857 [M−H]$^-$, 213.06, 124.96, 112.86	1.25	[21]
2	Protocatechuic acid	$C_7H_6O_4$	153.01824 [M−H]$^-$, 81.08, 108.84	1.56	[24]
3	Chlorogenic acid	$C_{16}H_{18}O_9$	353.08759 [M−H]$^-$, 191.01, 173.93	2.44	[24]
4	Paeoniflorin	$C_{23}H_{28}O_{11}$	479.15478	4.23	*
5	Isoorientin	$C_{21}H_{20}O_{11}$	447.09219 [M−H]$^-$, 327.04, 357.10, 429.20	4.76	[21]
6	Liquiritin apioside	$C_{26}H_{30}O_{13}$	549.16026 [M−H]$^-$, 417.22, 297.13, 255.15	6.11	[19]
7	Lithospermic acid	$C_{27}H_{22}O_{12}$	537.10275 [M−H]$^-$, 295.21, 493.21	7.46	[20]
8	Dicaffeoylquinic acid	$C_{25}H_{24}O_{12}$	515.11840 [M−H]$^-$, 190.93, 353.13	7.64	[23]
9	Rosmarinic acid	$C_{18}H_{16}O_8$	359.07614 [M−H]$^-$, 341.15, 160.93, 196.94, 179.02	8.56	[20]
10	Salvianolic acid B	$C_{36}H_{30}O_{16}$	717.14260 [M−H]$^-$, 519.22, 321.20	10.08	[20]
11	Quercetin	$C_{15}H_{10}O_7$	301.03427	11.05	*
12	Oleanoic acid	$C_{30}H_{48}O_3$	455.35197	35.31	*

* Compared with a standard. Other components were identified through comparison with m/z and mass fragmentation patterns reported in the literature

collagen synthesis in the presence of IL-1β through the MAPK signaling pathways that prevent P38, ERK, and JNK phosphorylation [14]. Phillyrin, an active ingredient extracted from forsythia, significantly inhibited receptor activator of nuclear factor κB ligand (RANKL)-induced osteoclastogenesis and bone resorption in vitro and protected against lipopolysaccharide-induced osteolysis in vivo. Phillyrin effectively blocked RANKL-induced activations of c-Jun N-terminal kinase and extracellular signal-regulated kinase, which suppressed the expression of c-Fos and nuclear factor of activated T-cells cytoplasmic 1 [15]. Imperatorin (IMT) reduced the release of TNF−α, IL-6 and IL-1β, inhibited the expression of iNOS and COX-2, and suppressed the activity of NF-κB
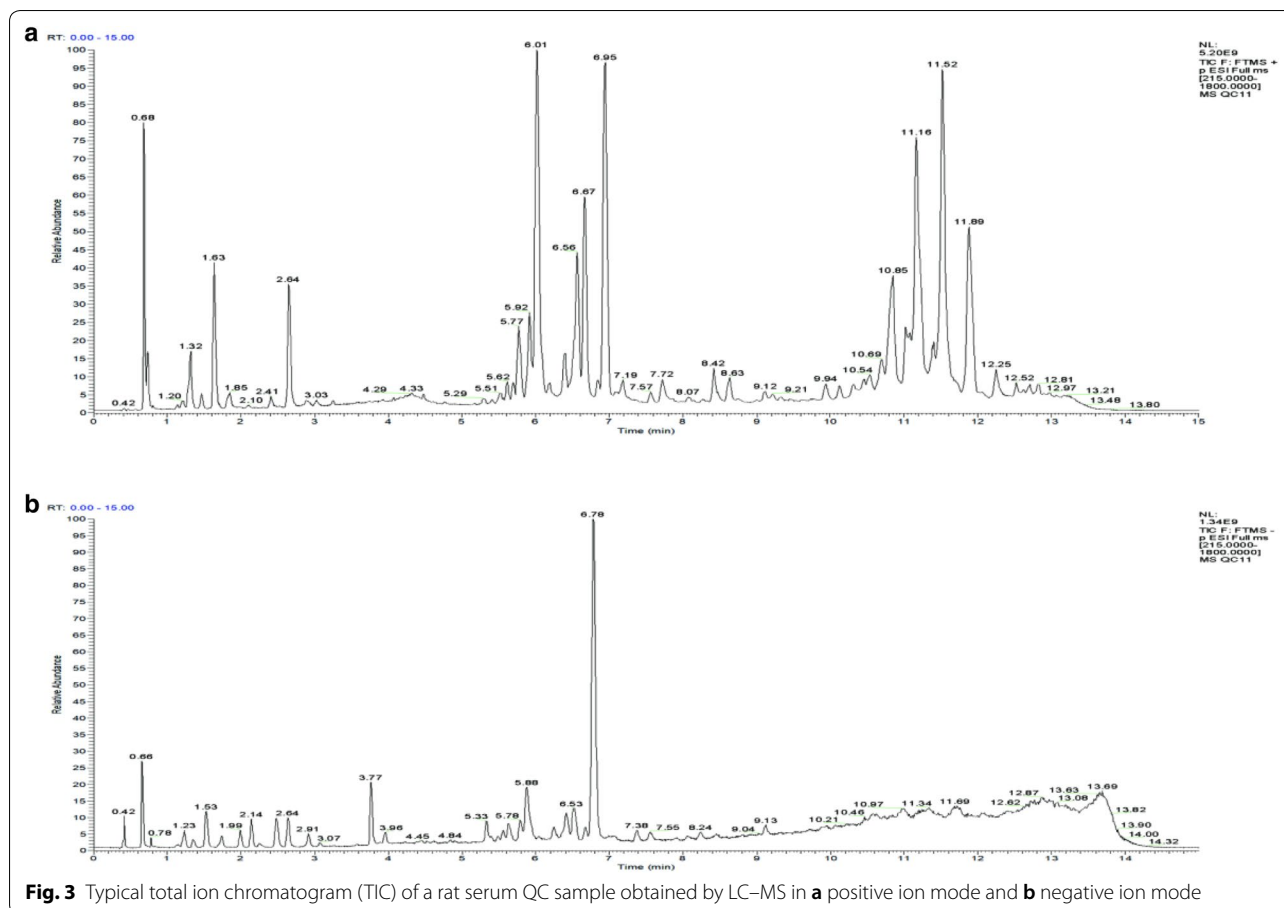
Wu *et al. Chin Med* (2020) 15:9

Page 8 of 13

Fig. 3 Typical total ion chromatogram (TIC) of a rat serum QC sample obtained by LC–MS in **a** positive ion mode and **b** negative ion mode

via upregulation of the expression of p65 (C) and IκB (C), and downregulation of the expression of p65 (N) [16]. Quercetin alleviated rat osteoarthritis by inhibiting inflammation and apoptosis of chondrocytes, modulating synovial macrophages polarization to M2 macrophages [17]. The pharmacological effects of Sanse powder may be a synergy of actions of multicomponents. Further studies are needed to elucidate the protective molecular mechanisms of Sanse powder on KOA in detail.

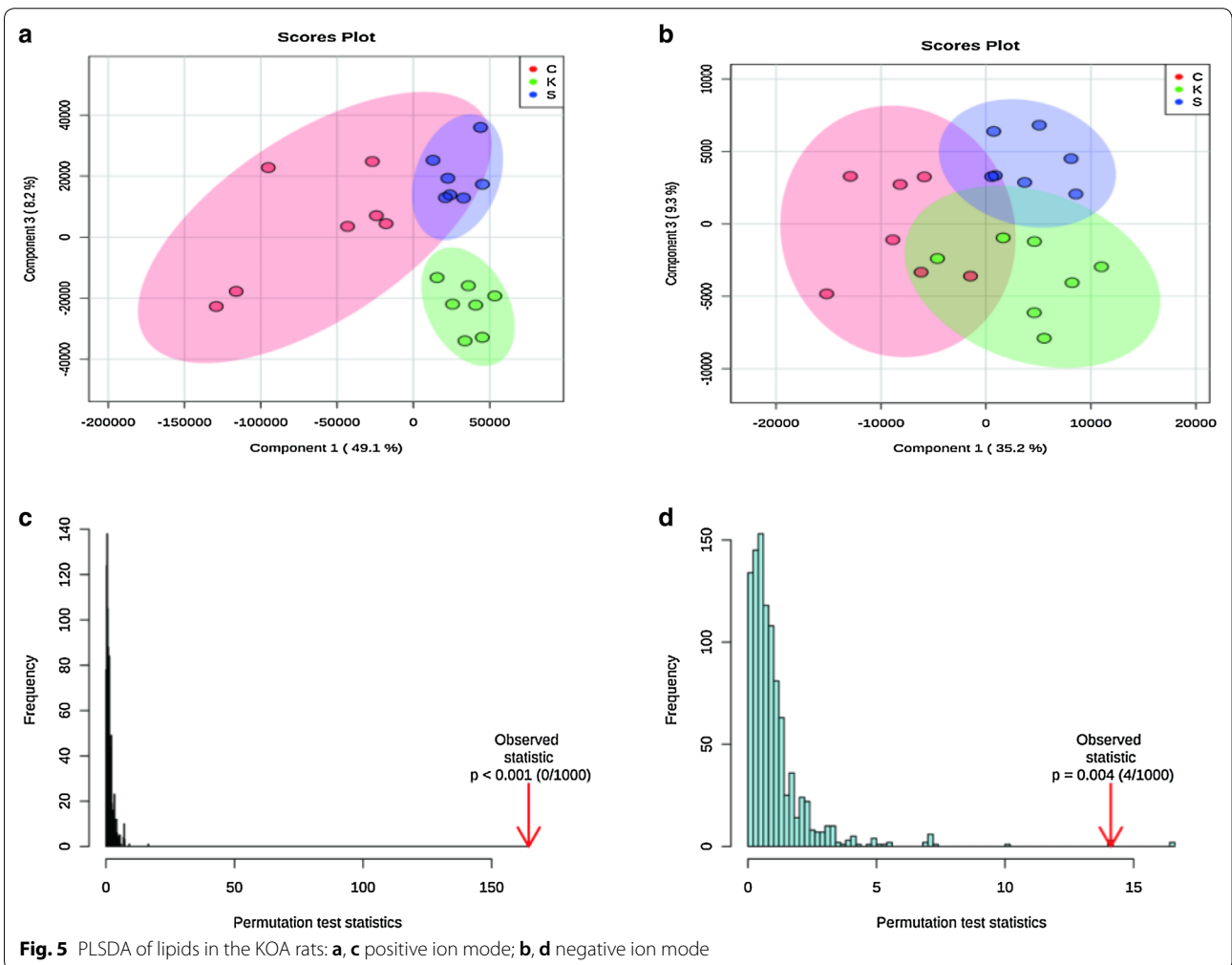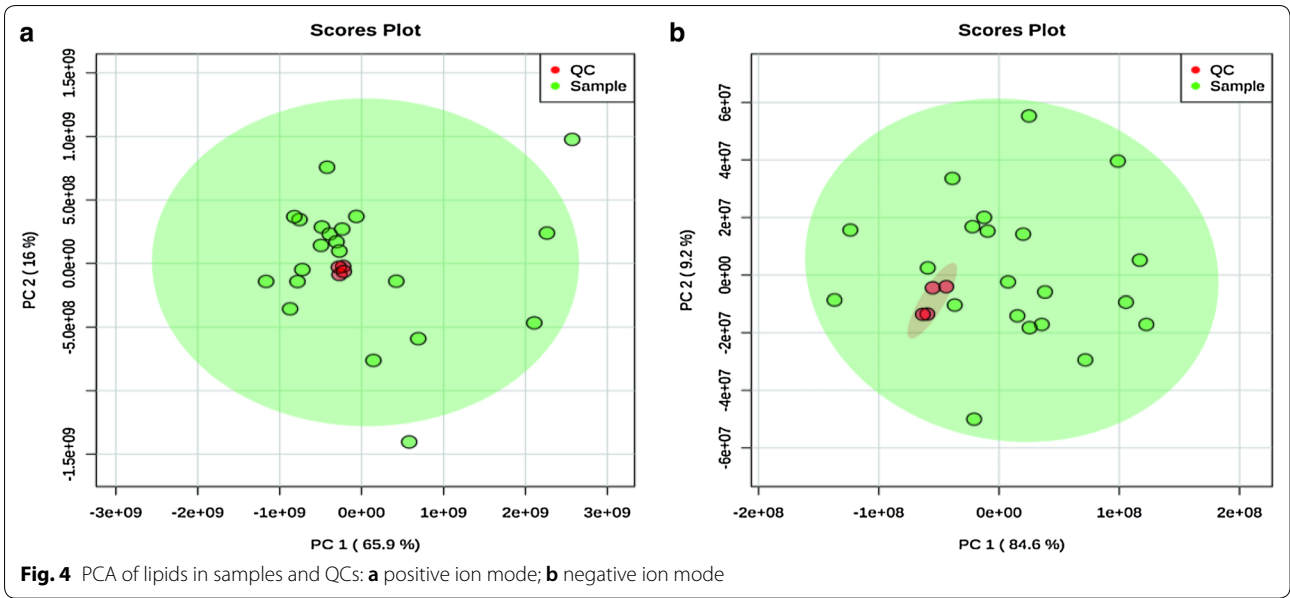### Lipid profile of rat serum
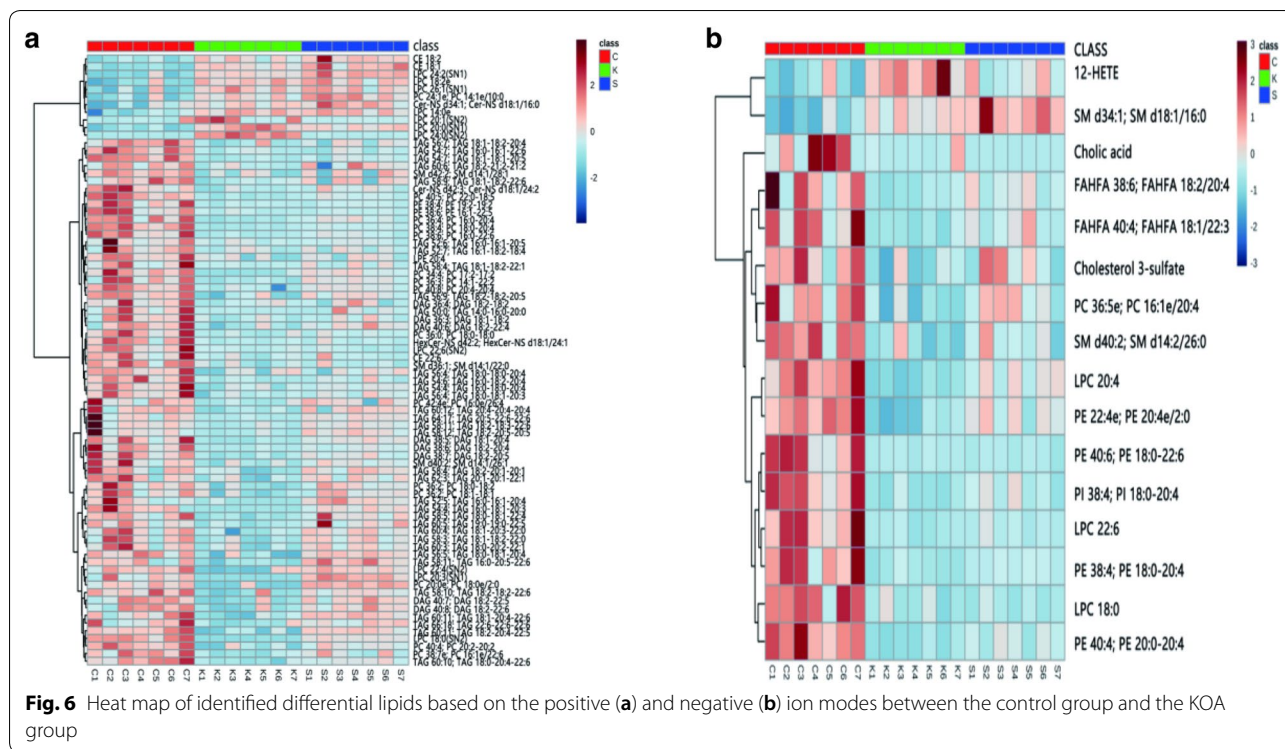#### *Total ion current map of rat serum (Fig. 3)*
Validation of the UPLC-Q-Exactive Orbitrap MS method Three methods were adopted to monitor the operating errors of the experiment and the stability of the instrument: (1) use of an advanced 5-pin QC sample balance system before injecting the experiment sample. (2) monitoring the peak height of the internal standards in all samples and then calculating their relatives standard deviations (RSDs) and (3) injecting a QC sample every 7 experimental samples. Principal component analysis of all samples, including the QC samples and the variation in

each substance in the QC samples were used to test the repeatability and reliability of the instrument.

To evaluate system stability and reproducibility, we used PLSDA analysis to process the data matrix of the QC samples. In the PLSDA score plots of the KOA samples, the QC samples were clustered by positive ionization and negative ionization which indicated that the stability of the LC–MS system was satisfactory throughout the analysis (Fig. 4). In addition, the RSDs of the internal standards, lyso-PE (17:1) and SM (17:0) in positive ion mode were 7.29% and 3.83%, respectively, and the RSD of lyso-PE (17:1) was 5.98% in negative ion mode.

Non-targeted lipidomics analysis The lipid metabolites in each group were divided according to ion modes: positive and negative. The data sets of each group for the positive and negative ion modes were analysed by PLSDA. Each point in Fig. 5 represents a sample. As shown in the figure, the control and the KOA groups showed significant separation, and the "Sanse powder" had a certain restorative effect; these effects were particularly evident in positive ion mode. The permutation test indicated that

Wu *et al. Chin Med* (2020) 15:9

Page 9 of 13

Fig. 4 PCA of lipids in samples and QCs: **a** positive ion mode; **b** negative ion mode

Fig. 5 PLSDA of lipids in the KOA rats: **a**, **c** positive ion mode; **b**, **d** negative ion mode

Wu *et al. Chin Med* (2020) 15:9

Page 10 of 13

Fig. 6 Heat map of identified differential lipids based on the positive (**a**) and negative (**b**) ion modes between the control group and the KOA group

the two PLSDA models were not over-fitted, indicating that the model is valid.

Analysis of lipid metabolites The KW-test and FDR calibration were used to identify the lipids in each group. $P < 0.05$ was considered to indicate significance for the differences in lipids between the control and KOA groups. And significance along with an FC > 1.5 denoted differential metabolites. Heat maps were used to showed the differential metabolites between the control and KOA groups (Fig. 6). Eighty metabolites in positive ion mode and 16 metabolites in negative ion mode were determined, but not all of these differential metabolites changed in the "Sanse powder" group. Therefore, we examined the differences in metabolites between the "Sanse powder" group and the KOA group by the same method. Thirty-four metabolites in positive ion mode and 2 metabolites in negative ion mode were found to differ between the groups, among which, 20 metabolites in positive ion mode and 2 metabolites in negative ion mode were also differentially expressed between the control and KOA groups. The restored lipids and the *P* values of the FCs are shown in Table 1.

Discussion

Lipid metabolism disorders can promote the occurrence and progression of OA via the effects of lipids on the degeneration of articular cartilage, synovitis, osteophyte

formation, bone marrow oedema, metabolism and the fluidity of cell membrane components [25]. Attaining a deeper understanding of the relationship between lipid composition and KOA can aid the identification of new targets for the treatment of diseases. Lipidomics is a rapidly evolving tool that explores the potential lipid biomarkers in diseases and the biological functions of lipids in various life activities by comparing the changes in lipid metabolism networks among different physiological conditions [26].

In our study, we observed that the prominent changes in KOA rats in TAGs, DAG, PC, LPC, PE, and FAHFAs, with the greatest change observed in TAGs. Most scholars consider KOA a systemic disease, and many studies have shown that there is a certain correlation between metabolic syndrome and OA, hypertension and that glucose and lipid metabolism disorders can promote the development of OA [27, 28]. Many studies have shown a positive correlations between both TAGs and DAG and KOA [29]: this finding was slightly unique, and that study contradicted this finding.

One major phospholipid component is PC, which plays a key role in maintaining physiological functions and normal metabolism of the body. PC is found in the brain, nervous system, liver, heart, kidneys, blood and other tissues and organs and is an important component of biofilm. PC participates in cell transport, oxidative phosphorylation, phagocytolysis, and chemical and electrical

Wu *et al. Chin Med* (2020) 15:9

Page 11 of 13

Table 2 Significantly changed metabolites in each group

Name	FC (KOA/control)	P. adjusted (KOA/control)	FC (Sanse powder/KOA)	P. adjusted (Sanse powder/KOA)
(A) Positive ion mode				
DAG 38:5; DAG 18:1-20:4	0.24397	0.00688	2.85705	0.00820
DAG 38:6; DAG 18:2-20:4	0.05126	0.00688	5.36171	0.01939
DAG 38:7; DAG 18:2-20:5	0.26403	0.00688	2.18564	0.02927
LPC 18:0(SN2)	0.08403	0.00688	6.48339	0.00820
LPC 20:3(SN1)	0.04763	0.00688	35.57942	0.00820
LPC 24:0(SN2)	10.12183	0.00688	0.15465	0.00820
PC 20:0e; PC 18:0e/2:0	0.01511	0.02103	84.63364	0.00820
PC 34:4; PC 17:2-17:2	0.10140	0.00688	5.27038	0.01939
PC 38:4; PC 18:0-20:4	0.20891	0.00688	1.54615	0.00820
TAG 52:5; TAG 16:0-16:1-20:4	0.03330	0.02103	35.65847	0.01669
TAG 54:4; TAG 16:0-18:0-20:4	0.04690	0.00688	13.83490	0.00820
TAG 56:5; TAG 18:0-18:1-20:4	0.28945	0.02103	2.73175	0.04829
TAG 58:11; TAG 16:0-20:5-22:6	0.46693	0.02103	2.37085	0.00820
TAG 58:12; TAG 18:2-20:5-20:5	0.53100	0.01641	2.04412	0.01422
TAG 58:3; TAG 18:1-18:2-22:0	0.62809	0.03199	1.52464	0.02927
TAG 60:10; TAG 18:0-20:4-22:6	0.29493	0.00688	1.88914	0.01939
TAG 60:11; TAG 18:1-20:4-22:6	0.66509	0.02103	1.53073	0.00820
TAG 60:11; TAG 18:2-20:4-22:5	0.07639	0.00688	12.63757	0.00820
TAG 60:4; TAG 18:1-20:3-22:0	0.56576	0.02103	1.64774	0.00820
TAG 64:17; TAG 20:5-22:6-22:6	0.02183	0.03199	36.57651	0.00820
(B) Negative ion mode				
FAHFA 40:4; FAHFA 18:1/22:3	0.13704	0.00869	2.15629	0.04779
PE 40:4; PE 20:0-20:4	0.34231	0.00683	1.56335	0.04779

excitation. In addition, PC is an important component of synovial fluid and cartilage and can inhibit cartilage hydration, scavenge oxygen free radicals and resist adhesion [30]. Several clinical studies and experiments have demonstrated that PC can alleviate the consequences of inflammation in different organs [31–33]. In general, PC can (1) reduce the interfacial tension and friction coefficient of articular cartilage, improve the physiological function of slide fluid, improve lubrication, and reduce cartilage wear; (2) reduce synovitis by controlling the synthesis and release of inflammatory mediators, such as IL-1β and TNF-α; and (3) inhibit the destruction of cartilage by inflammatory mediators in inflammatory joints, stimulate the synthesis of proteoglycan (PG), control the release of chondroitin-degrading enzymes, and accelerate the synthesis and metabolism of cartilage to stabilize and repair articular cartilage (Table 2).

LPCs also play an important role in inflammatory reactions [34], some studies suggest that the ratio of LPCs to PCs is closely related to KOA [35, 36]. Furthermore phospholipase A2 (PLA2) play a key role in this process [37]. In addition, PE, a type of phospholipid (PL), is an important component of articular cartilage [38]. In our study,

we found that the "Sanse powder" could restore PE levels. In addition, the concentration of FAHFAs decreased in the KOA group, which suggests that FAHFAs may play key roles in the knee joint. Therefore, the mechanisms underlying the effects of "Sanse powder" treatment on KOA may involve lipid metabolism disorders (Fig. 7).

Conclusions

In summary, our study confirmed that "Sanse powder" had pronounced protective effects against KOA in rats. "Sanse powder" can not only reduce synovitis but also improve the cold pain threshold and MWT. Additionally, the lipidomics results showed that the levels of TAGs, DAG, PC, LPC, FAHFAs and PE on KOA rats treated with "Sanse powder" were restored to almost normal levels.

The identification and analysis of lipids led us to hypothesized that lipid metabolism disorders occurred in the KOA rats and indicated that lipids play important roles in KOA. However, our study has limitations. The experiment was a non-target experiment, so although relative quantifications of the substances were obtained, the absolute levels of the analytes were not quantified.
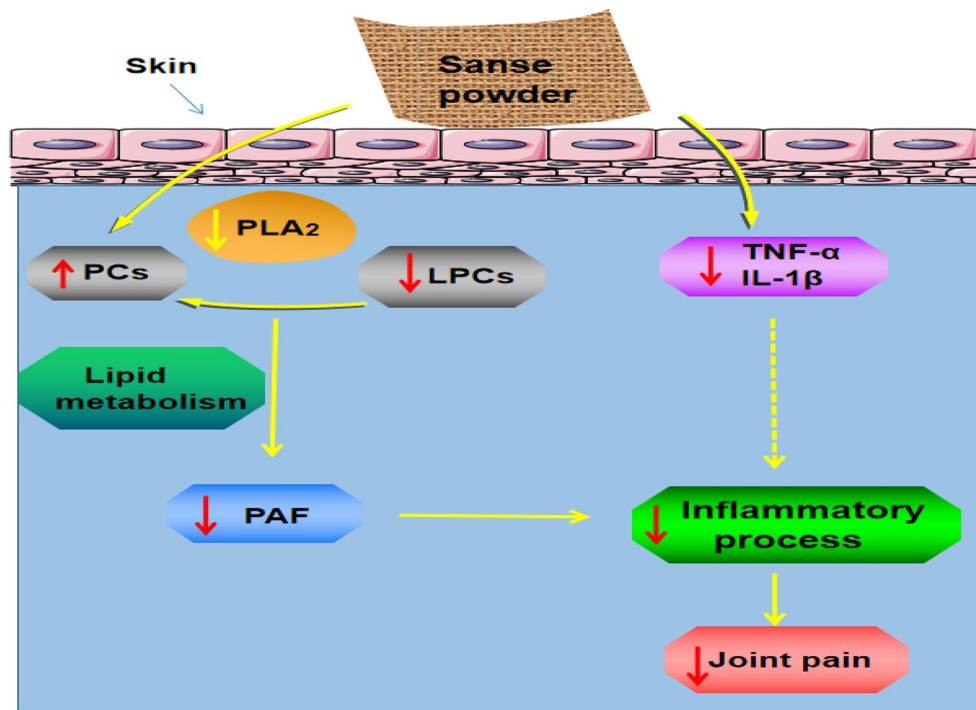
Wu *et al. Chin Med*   (2020) 15:9

Page 12 of 13

Fig. 7 The effects of "Sanse powder" on lipid levels in KOA. *PAF* platelet activating factor, *PLA2* phospholipase A2

Analyses of inflammation-related lipids in biological samples are necessary to explore their roles in cellular functioning and pathophysiological events.

Supplementary information

Supplementary information accompanies this paper at https://doi.org/10.1186/s13020-020-0290-5.

> **Additional file 1.** Animal ethics approval copy.

Abbreviations
KOA: knee osteoarthritis; MWT: mechanical withdrawal thresholds; H&E: haematoxylin and eosin; IL-1β: interleukin-1β; TNF-α: tumour necrosis factor-α; RT-qPCR: quantitative reverse transcription polymerase chain reaction; WB: western blot; UPLC-Q-Exactive Orbitrap MS: ultra-performance liquid chromatography combined with quadrupole-Exactive Orbitrap mass spectrometry; DAG: diacylglycerol; TAGs: triacylglycerols; LPC: lysophosphatidylcholine; PC: phosphatidylcholine; FAHFAs: fatty acid esters of hydroxy fatty acids; PE: phosphatidylethanolamine; NSAIDs: non-steroidal anti-inflammatory drugs; COX-2: cyclooxygenase 2; PGE2: prostaglandin E2; IMT: imperatorin; LC–MS: liquid chromatography–tandem mass spectrometry; CMMS: Chinese material medica; ACLT: anterior cruciate ligament transection; TIC: total ion chromatogram; RSDs: relative standard deviations; PAF: platelet activating factor; PLA2: phospholipase A2.

Authors' contributions
JJS, JM and PMW conceived the study and designed the experiments. ZQH participated in study design and drafted the manuscript. PW participated in data analysis, performed the statistical analysis and drafted the manuscript. PW, ZCL, SJY, YCX, and BX performed the KOA treatment, collected the samples and performed the experiments. NSZ, RLX, CSS, and WM participated in the literature searched and extracted the data. All authors read and approved the final manuscript.

Availability of data and materials
All data included in this article are available from the corresponding author upon request.

Ethics approval and consent to participate
The animal study was performed according to the International Rules Concerning Animal Experiments and the Internationally Accepted Ethical Principles for Laboratory Animal Use and Care.

Consent for publication
All authors have provided consent for publication in the journal of Chinese Medicine.

Competing interests
The authors declare that they have no competing interests.

Author details
[1] Affiliated Hospital of Nanjing University of Chinese Medicine, Nanjing 210029, China. [2] Jiangsu Province Hospital of Chinese Medicine, Nanjing 210029, China. [3] Medical Metabolomics Center, Nanjing University of Chinese Medicine, Nanjing 210023, China. [4] Jiangsu Key Laboratory of Pediatric Respiratory Disease, Institute of Pediatrics, Nanjing University of Chinese

Wu *et al. Chin Med*　　(2020) 15:9

Page 13 of 13

Medicine, Nanjing 210023, China. [5] Key Laboratory for Metabolic Diseases in Chinese Medicine, First College of Clinical Medicine, Nanjing University of Chinese Medicine, Nanjing 210023, China.

References

1. Davis JE, Ward RJ, Mackay JW, et al. Effusion-synovitis and infrapatellar fatpad signal intensity alteration differentiate accelerated knee osteoarthritis. Rheumatology. 2019;58(3):418–26.
2. Wallace G, Cro S, Dore C, et al. Associations between clinical evidence of inflammation and synovitis in symptomatic knee osteoarthritis: a cross-sectional substudy. Arthritis Care Res. 2017;69(9):1340–8.
3. Kan HS, Chan PK, Chiu KY, et al. Non-surgical treatment of knee osteoarthritis. Hong Kong Med J. 2019;25(2):127–33.
4. Guo B, Qin S, Ye H. Research progress of knee-salvage treatment for knee osteoarthritis. Zhongguo Xiu Fu Chong Jian Wai Ke Za Zhi. 2018;32(10):1292–6.
5. Rannou F, Pelletier JP, Martel-Pelletier J. Efficacy and safety of topical NSAIDs in the management of osteoarthritis: evidence from real-life setting trials and surveys. Semin Arthritis Rheum. 2016;45(4 Suppl):S18–21.
6. Li X. Mechanism of "Yiceng" external treatment of synovitis in knee osteoarthritis based on NLRP3/caspase-1 inflammatory corpuscle. Nanjing University of Traditional Chinese Medicine. 2018.
7. Wang Peimin, Yan Peijun, Ding Liang, et al. Clinical study on the treatment of acute soft tissue injury of ankle joint by yi layer application. J Nanjing Univ Tradit Chin Med. 2014;30(06):513–5.
8. Hyotylainen T, Ahonen L, Poho P, et al. Lipidomics in biomedical research-practical considerations. Biochim Biophys Acta Mol Cell Biol Lipids. 2017;1862(8):800–3.
9. Yang K, Han X. Lipidomics: techniques, applications, and outcomes related to biomedical sciences. Trends Biochem Sci. 2016;41(11):954–69.
10. Cajka T, Smilowitz JT, Fiehn O. Validating quantitative untargeted lipidomics across nine liquid chromatography-high-resolution mass spectrometry platforms. Anal Chem. 2017;89(22):12360–8.
11. Xing R, Wang P, Zhao L, et al. Mechanism of TRPA1 and TRPV4 participating in mechanical hyperalgesia of rat experimental knee osteoarthritis. Arch Rheumatol. 2017;32(2):96–104.
12. Yin S, Zhang L, Ding L, et al. Transient receptor potential ankyrin 1 (trpa1) mediates il-1beta-induced apoptosis in rat chondrocytes via calcium overload and mitochondrial dysfunction. J Inflflamm. 2018;15:27.
13. Jasmin L, Kohan L, Franssen M, et al. The cold plate as a test of nociceptive behaviors: description and application to the study of chronic neuropathic and pain models. Pain. 1998;75(2–3):367–82.
14. Zhao L, Ye J, Wu GT, et al. Gentiopicroside prevents interleukin-1 beta induced inflammation response in rat articular chondrocyte. J Ethnopharmacol. 2015;172:100–7.
15. Wang J, Chen G, Zhang Q, et al. Phillyrin attenuates osteoclast formation and function and prevents LPS-induced osteolysis in mice. Front Pharmacol. 2019;10:1188.
16. Zhang X, Li W, Abudureheman A, et al. Imperatorin possesses notable antiinflammatory activity in vitro and in vivo through inhibition of the NFkappaB pathway. Mol Med Rep. 2017;16(6):8619–26.
17. Hu Y, Gui Z, Zhou Y, et al. Quercetin alleviates rat osteoarthritis by inhibiting inflammation and apoptosis of chondrocytes, modulating synovial macrophages polarization to M2 macrophages. Free Radic Biol Med. 2019;145:146–60.
18. Qian W, Kang A, Peng L, et al. Gas chromatography-mass spectrometry based plasma metabolomics of H1N1-induced inflammation in mice and intervention with Flos Lonicerae Japonica-Fructus Forsythiae herb pair. J Chromatogr B Analyt Technol Biomed Life Sci. 2018;1092:122–30.
19. Rui F, Nan L, Jiang X, et al. HPLC–DAD–MS/MS identification and HPLC–ABTS•+ on-line antioxidant activity evaluation of bioactive compounds in liquorice (Glycyrrhiza uralensis Fisch.) extract. Eur Food Res Technol. 2015;240(5):1035–48.
20. Liang W, Chen W, Wu L, et al. Quality evaluation and chemical markers screening of *Salvia miltiorrhiza* Bge. (Danshen) based on HPLC fingerprints and HPLC-MSn coupled with chemometrics. Molecules. 2017;22(3):478.
21. Zekun ZH, Yaqi L, Zixuan W, et al. Rapid analysis of chemical constituents of 4 gentiana macrophylla strains by UPLC-LTQ-Orbitrap-MS. Zhongnan pharmacy. 2019;08:1–5.
22. Jiayu ZH, Qian ZH, Fan ZH, et al. Identification of four alkaloids in strychnine seeds by HPLC-ESI-MS-MS. Chin J Exp Formul. 2013;19(09):147–51.
23. Xin G, Wenjun S, Lin Q, et al. Rapid analysis of chemical constituents of ligusticun chuanxiong based on ultra-high performance liquid chromatography-electrospray-time-time-mass spectrometry. J Pharm. 2008;33(06):711–5.
24. Jieying SH, Honglei ZH, Qian ZH, et al. Analysis of chemical constituents of Chinese papaya decoction slices based on UPLC-Q-Exactive Orbitrap-MS. Chin Herb Med. 2008;49(20):4773–9.
25. Nano JL, Nobili C, Girard-Pipau F, et al. Effects of fatty acids on the growth of Caco-2cells. Prostaglandins Leukot Essent Fatty Acids. 2003;69(4):207–15.
26. Jinjun S, WenJuan Q, Cunsi S, et al. High-resolution lipidomics reveals dysregulation of lipid metabolism in respiratory syncytial virus pneumonia mice. RSC Adv. 2018;8(51):29368–77.
27. Sellam J, Berenbaum F. Is osteoarthritis a metabolic disease? Jt Bone Spine. 2013;80(6):568–73.
28. Zhai G. Alteration of metabolic pathways in osteoarthritis. Metabolites. 2019;9(1):11.
29. Futani H, Okayama A, Matsui K, et al. Relation between interleukin-18 and PGE2 in synovial fluid of osteoarthritis: a potential therapeutic target of cartilage degradation. J Immunother. 2002;25(Suppl 1):S61–4.
30. Hills BA, Thomas K. Joint stiffness and "articular gelling": inhibition of the fusion of articular surfaces by surfactant. Br J Rheumatol. 1998;37(5):532–8.
31. Eros G, Ibrahim S, Siebert N, et al. Oral phosphatidylcholine pretreatment alleviates the signs of experimental rheumatoid arthritis. Arthritis Res Ther. 2009;11(2):R43.
32. Elblehi SS, Hafez MH, El-Sayed YS. ʟ-alpha-Phosphatidylcholine attenuates mercury-induced hepato-renal damage through suppressing oxidative stress and inflammation. Environ Sci Pollut Res Int. 2019;26(9):9333–42.
33. Stremmel W, Haneman A, Braun A, et al. Delayed release phosphatidylcholine as new therapeutic drug for ulcerative colitis–a review of three clinical trials. Expert Opin Investig Drugs. 2010;19(12):1623–30.
34. Cui L, Lee YH, Kumar Y, et al. Serum metabolome and lipidome changes in adult patients with primary dengue infection[J]. PLoS Negl Trop Dis. 2013;7(8):e2373.
35. Zhang W, Sun G, Aitken D, et al. Lysophosphatidylcholines to phosphatidylcholines ratio predicts advanced knee osteoarthritis. Rheumatology. 2016;55(9):1566–74.
36. Zhai G, Pelletier JP, Liu M, et al. Activation of the phosphatidylcholine to lysophosphatidylcholine pathway is associated with osteoarthritis knee cartilage volume loss over time. Sci Rep. 2019;9(1):9648.
37. Pruzanski W, Bogoch E, Stefanski E, et al. Enzymatic activity and distribution of phospholipase A2 in human cartilage. Life Sci. 1991;48(25):2457–62.
38. Sarma AV, Powell GL, LaBerge M. Phospholipid composition of articular cartilage boundary lubricant. J Orthop Res. 2001;19(4):671–6.

Publisher's Note

Springer Nature remains neutral with regard to jurisdictional claims in published maps and institutional affiliations.